IEEE Access
Multidisciplinary | Rapid Review | Open Access Journal

Received December 25, 2019, accepted January 8, 2020, date of publication January 13, 2020, date of current version January 21, 2020.

Digital Object Identifier 10.1109/ACCESS.2020.2965965

Voltage/Var Control for Hybrid Distribution Networks Using Decomposition-Based Multiobjective Evolutionary Algorithm

FENG QIAO, (Student Member, IEEE), AND JIN MA, (Member, IEEE)
School of Electrical and Information Engineering, The University of Sydney, Sydney, NSW 2008, Australia
Corresponding author: Jin Ma (j.ma@sydney.edu.au)

ABSTRACT Hybrid distribution networks manage not only the traditional voltage/var controllers such as on-load tap changers and capacitor banks but also the independent entities such as grid-tied microgrids. Voltage/Var control (VVC) is challenging in this evolved system due to the difficulty of motivating the participation of various entities with conflicting interests. This paper proposes a multiobjective voltage/var optimisation model seeking tradeoff solutions to drive all the entities to maximise their VVC contributions. In the multiobjective VVC model, the contributions of different entities are identified by a fair resource allocation based approach. Moreover, the operational model of grid-tied hybrid AC/DC microgrid is integrated into the VVC to extend the application scenario to the future hybrid distribution network. The proposed VVC fairly identifies the contributions and adequately captures the tradeoffs among various independent entities, so their participation in VVC can be encouraged. The proposed multiobjective voltage/var optimisation model is solved by a genetic based solver called multiobjective evolutionary algorithm based on decomposition. The proposed VVC is tested on a modified IEEE 33 nodes system to demonstrate its effectiveness and advantages.

INDEX TERMS Fair resource allocation, hybrid distribution network, multi-objective optimization, voltage/var control.

NOMENCLATURE

C_i	Contribution in voltage/var control provided by entity i
C_Ω	Contribution in voltage/var control provided by all the entities
EP	External population
J	Set of on-load tap changers
K	Set of capacitor banks
L	Set of distributed generators in distribution network
M	Set of microgrids
N	Set of all the entities
S	Set of system buses
VQ	Node voltage quality
w_i	Action of entity i

PARAMETERS

ΔV	Maximum allowed node voltage deviation
η_{ch}	Charging cost coefficient of energy storage system
η_{dis}	Discharging cost coefficient of energy storage system
π	Reward coefficient
$\underline{*}, \overline{*}$	Lower and upper bound of variable *
B_{ij}	Susceptance of branch i-j
C_{ad}	Cost coefficient of interlinking converter in microgrid
C_{dg}	Cost coefficient of diesel generator in microgrid
C_{ess}	Cost coefficient of energy storage system in microgrid
C_{rg}	Cost coefficient of renewable generator in microgrid
dQ_{CBi}	Step size of capacitor bank at bus i
G_{ij}	Conductance of branch i-j
P_{load}	Load comsumption in microgrid
S_{DGi}	Converter's capacity of distributed generator i
S_{DGi}	Transformer's capacity of microgrid i
V_{rated}	Nominal voltage

The associate editor coordinating the review of this manuscript and approving it for publication was Hui Liu.

VARIABLES

$*^{AC}$	Variable * in AC subsystem of hybrid AC/DC microgrid
$*^{DC}$	Variable * in DC subsystem of hybrid AC/DC microgrid
α	Binary variable of diesel generator in microgrid
β	Binary variable of energy storage system in microgrid
η_i	Modulation rate of distributed generator i
γ	Binary variable of interlinking converter in microgrid
θ_{ij}	Voltage angle difference between bus i and j
k_i	Tap position of capacitor bank at bus i
P_{A2D}	Active power from AC subsystem to DC subsystem in microgrid
P_{ch}	Charging power of energy storage system in microgrid
P_{D2A}	Active power from DC subsystem to AC subsystem in microgrid
P_{DGi}	Active power of distributed generator i
P_{dis}	Discharging power of energy storage system in microgrid
P_{Li}	Active power consumption of load at bus i
P_{MGi}	Active power from microgrid i
P_{solar}	Active power of photovoltaic system in microgrid
P_{wind}	Active power of wind turbine generator in microgrid
Q_{CBi}	Reactive power of capacitor bank at bus i
Q_{DGi}	Reactive power of distributed generator i
Q_{Li}	Reactive power consumption of load at bus i
Q_{MGi}	Reactive power from microgrid i
SOC	State of charge of energy storage system
tap_i	Tap position of on-load tap changer i
V_i	Voltage of bus i

I. INTRODUCTION

The integration of electronically interfaced distributed generators (DGs) and microgrids (MGs) gives flexibility to distribution network operator (DNO) for satisfying the voltage/var control (VVC) objectives, which cover a wide range of operational issues including power loss reduction, coordination of different voltage/var resources, mitigation of unexpected voltage variation due to the varying operational modes of DGs and MGs. In traditional distribution networks, controllers such as on-load tap changers (OLTCs), capacitor banks (CBs), and DGs can be dispatched towards a global VVC objective. However, a hybrid distribution network becomes more diversified such that independent entities such as MGs could contribute to the VVC objectives along with other controllers by providing their ancillary power injections [1], [2]. It is necessary to clear the definition of 'controller' and 'entity' in this paper. The term 'controller' refers to a physically existing device that is capable of providing voltage/var support, i.e., an OLTC or a CB. The term 'entity' refers to an operator who may own multiple controllers and responsible for regulating these controllers contributing to the VVC objectives, i.e., an MG. In hybrid distribution networks, the challenge of VVC lies in not only the difficulty to co-manage different controllers but also the lack of a suitable motivation plan to encourage the participation of various entities. A reformed VVC scheme is required for this evolved system to rationally incorporate multiple entities with distinct operational interests.

Extensive research works address VVC problem in hybrid distribution networks by leveraging the controllability of the electronically interfaced DGs, which can be divided into three categories: centralised scheme [3]–[9], decentralised scheme [10]–[14], and distributed approach [15]–[21]. Moreover, the participation of MGs in VVC has been investigated in limited works. In [1], a centralised VVC is proposed to regulate voltage in a distribution network with multiple DGs and MGs. The optimisation is performed at the distribution network management system to calculate the set-points of OLTC, DGs, and MGs. The internal voltage and power loss in each MG is obtained via a pre-trained artificial neural network. In [22], a decentralised VVC is developed based on the multi-agent system. A game based method is utilised to reward MG's contribution by using Sharpley value. This method relies on a series of cost functions that can quantify the contributions provided by different sets of MGs' coalition. In [23], a two-stage distributed VVC is proposed to coordinate various VVC entities in a distribution network. The MG in which the voltage violation is sensed will call for help from neighbouring controllable entities. Then, these neighbouring entities update their set-points based on a cooperative distributed model predictive control algorithm.

For VVC problem in hybrid distribution networks, the following research gaps can be identified through the existing literature. First, it is required to create a reasonably acceptable motivation plan to reward different entities for their contributions. Consider that all the entities will have firm intention of maximising their contributions when DNO proposes to reward their participation, the motivation plan should address any possible conflicts among the entities when accommodating their contributions. Moreover, the contributions from various entities need to be identified before rewarding them. In a real system, different entities could interact with each other through the power flow; then, not only their actions but also their action sequences will lead to different voltage profiles in the system. We can accurately quantify their contributions only if we know their action sequences. Since this knowledge is not acquirable in practice, alternative identification methods need to be developed. Furthermore, the operational interests of different entities, including MGs, should be considered when designing an applicable VVC for future hybrid distribution networks. However, the participation of grid-tied MGs, especially for those with advanced structures such as the hybrid AC/DC MG [24], is rarely considered in the existing VVC schemes.

This paper targets the above research gaps, and its major contributions are as follows: 1) a multiobjective voltage/var optimisation model is formulated to find tradeoff solutions

for various VVC entities considering that their contributions cannot be simultaneously maximised; 2) an identification approach is developed based on fair resource allocation theory to identify the contributions provided by different VVC entities; 3) an integrated operational model for hybrid AC/DC MG is developed to extend the application scenario to future hybrid distribution networks.

This paper is organised as follows: Section 2 formulates the multiobjective VVC model and the integrated operational model of grid-tied hybrid AC/DC MG. Section 3 develops a fair resource allocation based approach to identify the contributions from various entities; Section 4 introduces a genetic-based solver called multiobjective evolutionary algorithm based on decomposition and illustrates the computation procedures of the proposed VVC. In Section 5, case studies are carried out on a modified IEEE 33 nodes system to show the effectiveness and merits of the proposed method.

II. MULTIOBJECTIVE VOLTAGE/VAR OPTIMISATION MODEL

In traditional distribution networks, VVC objectives are usually achieved by dispatching all the controllers through a single objective optimisation model. However, the controllers may belong to different entities in a hybrid distribution network, which makes the traditional VVC inapplicable. The entities in hybrid distribution networks usually receive certain rewards in proportion to their contributions. Under this scenario, all the entities have a strong intention to maximise their contributions. However, increasing or decreasing one's contribution should be determined according to whether this dispatch can help to improve the voltage quality. Besides, possible conflicts could occur when increasing one's contribution will lead to the decrease of others'. Thus, the primary purpose of designing the VVC for hybrid distribution networks should be seeking trade-offs when dispatching various entities. To this end, the following multiobjective VVC model is developed to find tradeoff solutions maximising the contributions provided by different entities.

A. OBJECTIVES OF MULTIOBJECTIVE VOLTAGE/VAR OPTIMISATION MODEL

The multiobjective optimization (MOO) problem is formulated in (1). In this paper, DNO is treated as an entity who can control OLTCs, CBs and DGs in the system, and each MG is treated as an independent entity who can manage its local devices such as renewable DGs and energy storage systems (ESSs). The objective f_i in (1) represents the contribution from the ith entity. For example, $f_i = C_i(x, u)$ could be the contribution provided by an MG from controlling its local devices.

Under the multiobjective model (1), any entity cannot increase its contribution by decreasing others'. Then, the conflicts when all the entities intent on simultaneously maximising their contributions can be thoroughly addressed, which makes the model applicable in a hybrid distribution network.

$$\begin{aligned} &\max\{f_1, f_2, \ldots, f_N\} \\ &f_i = C_i(x, u), \quad i = 1, 2, \ldots, N \end{aligned} \tag{1}$$

The term x represents all the state variables such as node voltages and power flows, and u represents all the decision variables. For the VVC in a hybrid distribution network, the decision variables include tap positions of OLTCs and CBs, and set-points of DGs and MGs. Since the DGs and MGs investigated in this paper electronically interface to the system, their set-points include both active and reactive power. It should be noted that the reactive power control from a DG is constrained by its active power output; thus, the total capacity limit is not violated. This cross-constrained complexity is captured in our model, which optimises both the active power and reactive power outputs. The constraints for the system operation are described in the following section.

B. HYBRID DISTRIBUTION NETWORK CONSTRAINTS

The equality constraints for a hybrid distribution network are defined in (2), which include active and reactive power balance of each bus and reactive power provided by CBs. The term k_i is tap position of the ith CB, and dQ_{CBi} is step size of the ith CB. For the buses that are not connected by a DG, an MG, or an CB, the corresponding terms set as zero in the model.

$$\begin{cases} P_{DGi} + P_{MGi} - P_{Li} \\ = V_i \sum_{j=1}^{S} V_j (G_{ij} \sin\theta_{ij} + B_{ij} \cos\theta_{ij}) \\ Q_{DGi} + Q_{MGi} + Q_{CBi} - Q_{Li} \\ = V_i \sum_{j=1}^{S} V_j (G_{ij} \sin\theta_{ij} - B_{ij} \cos\theta_{ij}) \\ Q_{CBi} = k_i dQ_{CBi} \end{cases} \tag{2}$$

The inequality constraints in (3) denote operational limits for node voltage and adjustment ranges of OLTCs and CBs. The adjustment ranges of OLTCs and CBs can be predefined by their technical characteristics.

$$\begin{cases} \underline{V} \le V_i \le \overline{V} \\ \underline{\theta} \le \theta_i \le \overline{\theta} \\ \underline{tap_i} \le tap_i \le \overline{tap_i} \\ 0 \le k_i \le \overline{k_i} \end{cases} \tag{3}$$

The constraints of power generation from DGs and MGs are denoted in (4). The active power generation from a DG can be controlled according to its predicted maximum active power generation and the modulation rate η_i. The modulation rate η_i is a discrete variable which can be ranging from its lower to upper bounds. The reactive power generation from a DG is restricted by its active power output and its converter's capacity. The active power injection of an MG P_{MGi} can be tuned within the range provided by MG's operational model.

The reactive power injection of an MG Q_{MGi} can be adjusted concerning its active power injection and the capacity of its transformer.

$$\begin{cases} P_{DGi} = \eta_i \overline{P_{DGi}} \\ \underline{\eta_i} \le \eta_i \le \overline{\eta_i} \\ Q_{DGi}^2 \le (S_{DGi})^2 - (P_{DGi})^2 \\ \underline{P_{MGi}} \le P_{MGi} \le \overline{P_{MGi}} \\ Q_{MGi}^2 \le (S_{MGi})^2 - (P_{MGi})^2 \end{cases} \tag{4}$$

C. HYBRID AC/DC MICROGRID OPERATION MODEL

Figure 1 shows the hybrid AC/DC MG investigated in this paper. It consists of diesel generators, wind generator, photovoltaic (PV) system and ESSs. All of these devices interface to the MG via electronic converters. Besides, an interlinking converter is equipped between its AC and DC subsystem and a solid-state transformer is connected between its AC subsystem and the distribution network.

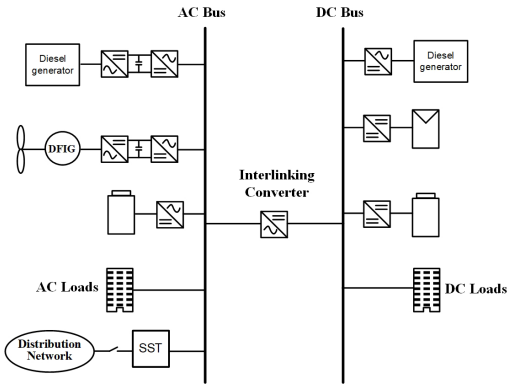

FIGURE 1. Schematic diagram of hybrid ac/dc microgrid.

For each time interval, the upper and lower boundaries of MG's active power injection can be obtained by calculating maximal and minimal local power generation, and it cannot exceed the capacity of the transformer. The boundaries are provided to the MOO model as parameters. Then, the setpoints for all the entities in the system can be determined, including P_{MG} and Q_{MG}. After P_{MG} and Q_{MG} are determined, optimisation problem (5) is solved to minimise the operational cost and calculate the setpoints for all the local devices in MG. The cost coefficient C_{rg} in (5) is set as negative to ensure the renewable generation can be only adjusted after all the other power sources are fully loaded.

$$\begin{aligned} \min J = {} & C_{dg}(P_{DG}^{AC} + P_{DG}^{DC}) \\ & + C_{ess}(P_{dis}^{AC} + P_{dis}^{DC}) \\ & + C_{ess}(P_{ch}^{AC} + P_{ch}^{DC}) \\ & + C_{rg}(P_{wind}^{AC} + P_{solar}^{DC}) \\ & + C_{ad}(P_{A2D} + P_{D2A}) \end{aligned} \tag{5}$$

The operational constraints of MG are defined in the following. The equality constraints in (6) denote the power balance in AC and DC subsystems.

$$\begin{cases} P_{DG}^{AC} + P_{dis}^{AC} - P_{ch}^{AC} + P_{wind}^{AC} - P_{load}^{AC} \\ = P_{A2D} - P_{D2A} + P_{MG} \\ P_{DG}^{DC} + P_{dis}^{DC} - P_{ch}^{DC} + P_{solar}^{DC} - P_{load}^{DC} \\ = P_{D2A} - P_{A2D} \end{cases} \tag{6}$$

The inequality constraints in (7) denote the operational limits for the diesel generators. The binary variables α_{DG}^{AC} and α_{DG}^{DC} are utilised to control the on and off state of the diesel generators.

$$\begin{cases} \alpha_{DG}^{AC} \underline{P_{DG}^{AC}} \le P_{DG}^{AC} \le \alpha_{DG}^{AC} \overline{P_{DG}^{AC}} \\ \alpha_{DG}^{DC} \underline{P_{DG}^{DC}} \le P_{DG}^{DC} \le \alpha_{DG}^{DC} \overline{P_{DG}^{DC}} \end{cases} \tag{7}$$

The operational limits of the ESSs are denoted in (8). The binary variables β_{dis} and β_{ch} control the ESSs to be operated in either charging or discharging state. The power loss during charging and discharging is considered in the model by setting η_{ch} and η_{dis} as charging and discharging cost coefficients. The state of charge of the ESSs is limited by the corresponding lower and upper boundaries.

$$\begin{cases} \beta_{dis}^{AC} \underline{P_{dis}^{AC}} \le P_{dis}^{AC} \le \beta_{dis}^{AC} \overline{P_{dis}^{AC}} \\ \beta_{ch}^{AC} \underline{P_{ch}^{AC}} \le P_{ch}^{AC} \le \beta_{ch}^{AC} \overline{P_{ch}^{AC}} \\ \beta_{dis}^{AC} + \beta_{ch}^{AC} \le 1 \\ \underline{SOC^{AC}} \le SOC^{AC} - \dfrac{P_{dis}^{AC}}{\eta_{dis}^{AC}} + \eta_{ch}^{AC} P_{ch}^{AC} \le \overline{SOC^{AC}} \\ \beta_{dis}^{DC} \underline{P_{dis}^{DC}} \le P_{dis}^{DC} \le \beta_{dis}^{DC} \overline{P_{dis}^{DC}} \\ \beta_{ch}^{DC} \underline{P_{ch}^{DC}} \le P_{ch}^{DC} \le \beta_{ch}^{DC} \overline{P_{ch}^{DC}} \\ \beta_{dis}^{DC} + \beta_{ch}^{DC} \le 1 \\ \underline{SOC^{DC}} \le SOC^{DC} - \dfrac{P_{dis}^{DC}}{\eta_{dis}^{DC}} + \eta_{ch}^{DC} P_{ch}^{DC} \le \overline{SOC^{DC}} \end{cases} \tag{8}$$

The inequality constraints in (9) are operational limits for the interlinking converter and the solid-state transformer (SST). The binary variables γ_{A2D} and γ_{D2A} are used to control the power direction between AC and DC subsystem.

$$\begin{cases} \gamma_{A2D} \underline{P_{A2D}} \le P_{A2D} \le \gamma_{A2D} \overline{P_{A2D}} \\ \gamma_{D2A} \underline{P_{D2A}} \le P_{D2A} \le \gamma_{D2A} \overline{P_{D2A}} \\ \gamma_{A2D} + \gamma_{D2A} \le 1 \\ \underline{P_{MG}} \le P_{MG} \le \overline{P_{MG}} \end{cases} \tag{9}$$

III. IDENTIFICATION OF VOLTAGE/VAR CONTRIBUTION

Applying the MOO model formulated in II requires an explicit form to represent the contribution provided by each entity. In this section, contribution in VVC is defined first, and the challenge to identify the contribution is ascertained. Finally, an identification approach is developed based on the fair resource allocation theory to determine the contribution provided by each entity.

A. CONTRIBUTION IN VOLTAGE/VAR CONTROL

In a hybrid distribution network with high penetration of DGs and MGs, it is often required to maintain the node voltages as much close to the rated value as possible to keep the system robust for accommodating the intermittent output of DGs and various operation modes of MGs. Therefore, the contribution in VVC is modelled according to the node voltage quality. The node voltage quality of an S-node system can be quantified by (10), where V_{rated} is the nominal voltage of the system and ΔV is the maximum allowed node voltage deviation (e.g. ΔV could be 0.05 p.u. if maximum 5% voltage deviation is permitted).

$$VQ = \sum_{i=1}^{S} \left(\frac{|V_i - V_{rated}|}{\Delta V}\right) \tag{10}$$

The total contribution from all the entities can be obtained by (11), in which VQ_0 is the node voltage quality in the base case where all the entities are deactivated, and VQ_Ω is the node voltage quality when all the entities participate in VVC. The term w_i represents the action of the ith entity. For example, w_i could be the action of an MG, which includes the adjustment actions of all its local devices.

$$\begin{aligned} C_\Omega &= \pi(VQ_0 - VQ_N) \\ &= \pi[VQ_0 - VQ(\omega_1, \omega_2, \ldots, \omega_i, \ldots, \omega_N)] \end{aligned} \tag{11}$$

The term π is a reward coefficient which can be pre-defined by DNO. A reasonable π could be determined by DNO to encourage independent entity's participation to achieve a satisfying voltage quality. For example, if the maximum allowed node voltage deviation is set as 0.05 pu, and only one node is considered. All the entities could share 2π reward from DNO if their participations help to improve the node voltage quality from 1.1 to 1 pu.

B. IDENTIFYING CONTRIBUTION OF INDIVIDUAL ENTITY

Although the total contribution as defined in (11) can be easily obtained by running two successive calculations with and without entities' participation, identifying any individual entity's contribution is challenging. This challenge lies in the fact that different action order of an entity could result in different value of its contribution. Simulation was carried out on a test system with eight entities to demonstrate this issue. In the simulation, the action order of the ith entity is set from the first to the last, and its corresponding contributions are shown in Figure 2. In the figure, $C^1_{\omega_i}$ calculated by (12) represents the contribution provided by the ith entity if it is the first one adding to the system, while $C^N_{\omega_i}$ calculated by (13) represents its contribution if it is the last one adding to the system. Here, we assume the reward coefficient π is one to facilitate the analysis.

$$C^1_{\omega_i} = VQ_0 - VQ(\omega_i) \tag{12}$$

$$C^N_{\omega_i} = VQ(\omega_1, \ldots, \omega_{N-1}) - VQ(\omega_1, \omega_2, \ldots, \omega_{N-1}, \omega_i) \tag{13}$$

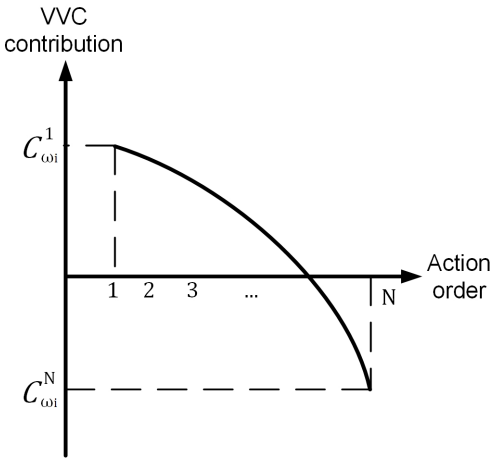

FIGURE 2. Impact of different action orders of the ith entity on its voltage/var control contribution (N = 8).

Figure 2 shows that the contribution provided by an individual entity could decrease if it is added to the system later rather than earlier. Due to the non-linearity of the power flow calculation and the cross-influence among multiple entities, the illustrated feature inevitably exists in a system. Identifying entities' contributions can be accurate only if their action sequences are known, which is, however, not viable in practice. Hence, an identification method doesn't require the knowledge of action sequences is required.

C. IDENTIFICATION APPROACH BASED ON FAIR RESOURCE ALLOCATION

In this subsection, an identification approach is developed based on the theory of fair resource allocation [25], [26], which can fairly identify the contribution of each entity without knowing their action sequences.

The total contribution calculated by (11) can be fairly distributed to the N entities by solving the optimisation problem as formulated in (14). The optimisation model (14) can be treated as a special form of fair resource allocation problem that fairly distributes the total contribution C_Ω to the N entities. According to (14), the ith entity's contribution is represented by C_{ω_i}, and the distance from C_{ω_i} to $C^1_{\omega_i}$ and from C_{ω_i} to $C^N_{\omega_i}$ is minimised. It indicates that using C_{ω_i} provides a fairest approach to quantify the contribution provided by the ith entity without the knowledge of the action sequences.

$$\begin{aligned} &\min \sum_{i=1}^{N} [(C_{\omega_i} - C^1_{\omega_i})^2 + (C^N_{\omega_i} - C_{\omega_i})^2] \\ &s.t. \sum_{i=1}^{N} C_{\omega_i} = C_\Omega \end{aligned} \tag{14}$$

$$C_{\omega_i} = \frac{1}{2}(C^1_{\omega_i} + C^N_{\omega_i}) + \frac{\lambda}{4} \tag{15}$$

The optimal solution of (14) can be calculated by the Lagrangian method, which is shown in (15). The first term

in (15) is the average value of $C^1_{\omega_i}$ and $C^N_{\omega_i}$, which is indeed a point between $C^1_{\omega_i}$ and $C^N_{\omega_i}$ in Figure 2. The value of this term can be easily determined by applying (12) and (13). The second term in (15) is a small mismatch generated by the Lagrangian multiplier λ, which can be calculated by (16) after the first terms and the total contribution are determined.

Using (15) can explicitly represent the contribution of any individual entity. Then, the MOO model proposed in II can be applied with the identified contribution of each entity.

$$\frac{\lambda}{4} = \frac{C_\Omega - \sum_{i=1}^{N}(\frac{C^1_{\omega_i}+C^N_{\omega_i}}{2})}{N}, \quad i = 1, \ldots, N \tag{16}$$

IV. SOLUTION METHOD

A. MULTIOBJECTIVE EVOLUTIONARY ALGORITHM BASED ON DECOMPOSITION

The MOO VVC model formulated in Section II aims to find trade-off solutions among multiple objectives, which can be solved by utilising the concept of Pareto optimal [27]. Since the formulated MOO problem has high nonlinearity and discrete features, it is challenging to solve it by using a mathematics-based approach, such as the weighted sum method [28]. In this paper, a genetic-based solver called multiobjective evolutionary algorithm based on decomposition (MOEA/D) [29] is employed. MOEA/D solves a series of sub-optimisation problems instead of the original optimisation problem to seek Pareto solutions. Since only a few information of neighbouring sub-problems are required to solve each sub-problem in each iteration, MOEA/D outperforms other MOO solvers such as NSGA II [30] and MOGLS [31] by its lower computational complexity.

The first step of MOEA/D is to decompose the original MOO problem (1). In this paper, decomposition of (1) is achieved by Tchebycheff approach. For an N-objective optimization problem, an N-dimension vector $\lambda = (\lambda_1, \ldots, \lambda_N)$ is required for the decomposition. If the number of sub-problems is R, a set of evenly spread weight vectors $[\lambda^1 = (\lambda^1_1, \ldots, \lambda^1_N), \ldots, \lambda^S = (\lambda^R_1, \ldots, \lambda^R_N)]$ is required. Then, R scalar optimization sub-problems can be decomposed from the original problem, and the objective function of the *ith* sub-problem is

$$\min g^{te}(x|\lambda^i, z^*) = \max_{1\le k\le N} \lambda^i_k |f_k(x,u) - z^*_k| \tag{17}$$

where $z^*_1, \ldots, z^*_N$ are reference values, i.e., $z^*_i = \max f_i(x,u)$ for each $i = 1, \ldots, N$. Since g^{te} is continuous of λ, the optimal solution of $g^{te}(x|\lambda^i, z^*)$ is close to that of $g^{te}(x|\lambda^j, z^*)$ if the Euclidean distance between weight vectors λ^i and λ^j is close to each other. The $g^{te}(x|\lambda^i, z^*)$ can be optimised by searching the weight vectors close to λ^i. Thus, all the R sub-problems can be optimised simultaneously in a single run based on their corresponding weight vectors. The major steps of MOEA/D are introduced below in Table 1. The genetic operator in Step 3.1 includes an one-point crossover stage and a standard mutation stage, as suggested in [29]. The Pareto solutions found in each iteration are stored in an external population *EP* for the decision-making stage.

TABLE 1. MOEA/D steps.

Step 1 Input parameters and data
Step 2 Initialization of MOEA/D *Step 2.1* Generate R evenly spread weight vectors, and initialise the external population EP. *Step 2.2* Compute the Euclidean distance between any two weight vectors, find the T closest weight vectors for each vector. For ith weight vector λ^i, store the indexes of its T closest weight vectors as $B_i = \{i_1, ..., i_T\}$. *Step 2.3* Randomly generate R initial solutions $u_1, u_2, ..., u_R$ with respect to the constraints defined in Section III. Calculate each objective value in (1) by applying (15). *Step 2.4* Initialise $z = (z_1, z_2, ..., z_i, ..., z_N)$, in which z_i is the maximal value of f_i found in above initial solutions.
Step 3 Update For i = 1,2,...,R *Step 3.1 Reproduction* Randomly select two indexes i_k and i_l from B_i, then generate a new solution y by using x_k and x_l through a genetic operator. *Step 3.2 Constraints Checking for Decision Variables* Check y by using the constraints defined in section III, replace any elements in y with its corresponding upper or lower bound if its upper or lower bound is affected. *Step 3.3 Update of z* For each $j = 1, ..., N$, update z_j with $f_j(y)$ if $z_j < f_j(y)$. *Step 3.4 Update of Neighbouring Solutions* For each index j in B_i, set $x_j = y$ and $FV^j = F(y)$ if $g^{te}(y|\lambda^j, z) \le g^{te}(x_j|\lambda^j, z)$. *Step 3.5 Update of EP* Remove from EP all the solutions dominated by $F(y)$, and add $F(y)$ to EP if no solutions in EP dominate $F(y)$. *Step 3.6 System Constraints Checking* Remove from EP all the solutions violate the constraints in (3).
Step 4 Stopping Criteria Checking If the maximum iteration number is reached, stop and output EP. or go to Step 3.

B. CODING PRINCIPLE

For a system with J OLTC, K CBs, L DGs, and M MGs, the length of an individual solution is $J + K + L + M$. Table 2 shows a sample for an individual coded solution. The first $J + K + L$ digits are discrete variables, while the rest are continuous variables. All the variables are heuristically changing during the MOEA/D calculation concerning their permitted ranges. It is worth noting that the permitted range of Q_{DG} and Q_{MG} can be only determined after P_{DG} and P_{MG} are chosen, thus, the allowed range for Q_{DG} and Q_{MG} are dynamically updated with respect to the changing values of P_{DG} and P_{MG} during each iteration.

TABLE 2. Sample of an individual coded solution.

tap_1	tap_2	...	tap_{J-1}	tap_J
k_1	k_2	...	k_{K-1}	k_K
η_1	η_2	...	η_{L-1}	η_L
Q_{DG_1}	Q_{DG_2}	...	$Q_{DG_{L-1}}$	Q_{DG_L}
P_{MG_1}	P_{MG_2}	...	$P_{MG_{M-1}}$	P_{MG_M}
Q_{MG_1}	Q_{MG_2}	...	$Q_{MG_{M-1}}$	P_{MG_M}

C. DECISION-MAKING

Applying MOEA/D gives multiple Pareto solutions, and each represents certain trade-offs among contributions of the entities. A problem specified decision-making stage is required to make a unique decision for the final execution. Various decision-making methods are proposed, such as graphical

based method [32] and fuzzy theory-based method [33], [34]. In this paper, the maximisation problem, as shown in (18) is used to make a decision, where U denotes the solution space constituted by all the Pareto solutions. By applying (18), the total contribution from all the entities are maximised in the decision-making stage.

$$\arg\max_{u\in U} J(u) = \sum_{i=1}^{N} C_{\omega_i}(u) \tag{18}$$

D. PROCEDURES OF THE VOLTAGE/VAR CONTROL SCHEME

The flow chart in Figure 3 illustrates the computation procedures of the proposed VVC. For each time interval, the upper and lower boundaries of MGs' active power injection are determined by each MG. Then, the boundaries are sent to DNO to execute the MOO model for calculating the setpoints of all the controllers. Finally, DNO sends the determined P_{MG} and Q_{MG} to each MG to calculate the set-points of its local devices.

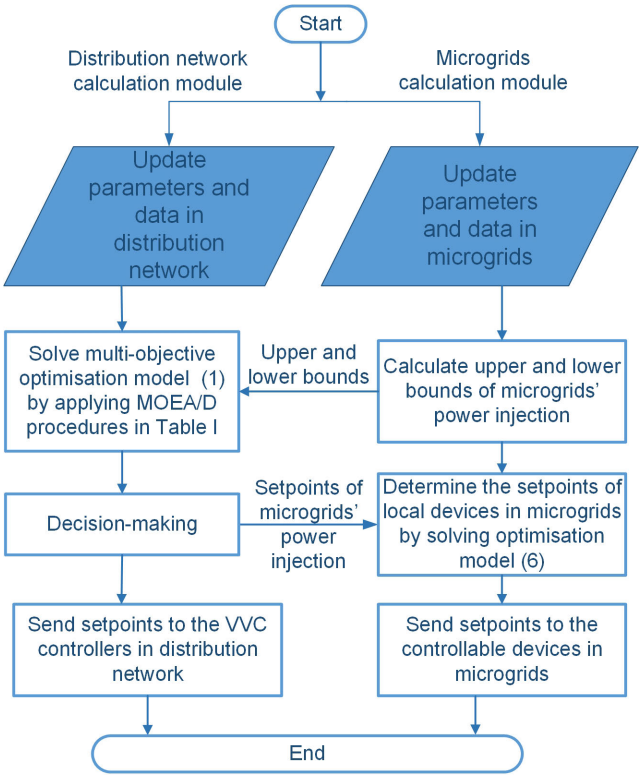

FIGURE 3. Implementation of VVC algorithms.

V. CASE STUDY

A. HYBRID DISTRIBUTION NETWORK DESCRIPTION

Figure 4 illustrates the investigated hybrid distribution network. The system is modified based on the one initially used in [35]. The maximum allowed bus voltage deviation is 0.05 pu. In the modified system, OLTC controls the secondary voltage of substation transformer, which is represented by bus 1. The OLTC has 20 tap positions that is capable

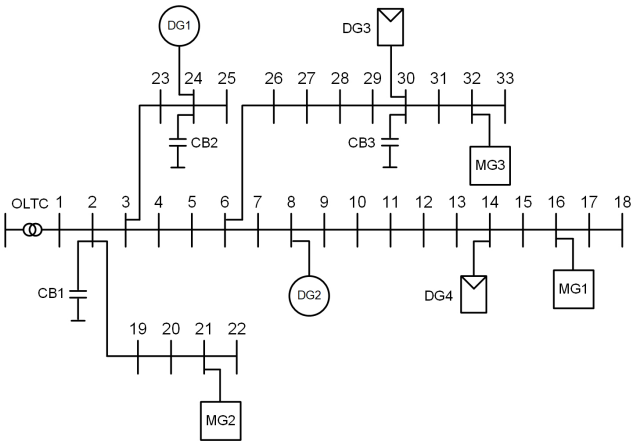

FIGURE 4. Test system.

of controlling the secondary voltage ranging from 0.95 to 1.05 pu. All the CBs have three steps, and provide reactive power compensation for 0.1 MVAr per step. Besides, there are two wind turbine generators located at bus 24 and 8 and two PV systems located at bus 30 and 14. These renewable DGs connect to the distribution network via electronic converters, and the maximum capacities of the converters are 3, 2, 1.5 and 1 MVA, respectively. The maximum modulation rate for renewable DGs is set as 50%. In addition, three hybrid AC/DC MGs are installed at bus 16, 21 and 32, and they have the same configurations as shown in Table 3.

TABLE 3. Configurations of Hybrid AC/DC Microgrid.

DC subsystem		
Diesel generator	Maximum generation	1 MW
PV system	Maximum generation	1.5 MW
Load	Maximum consumption	1.5 MW
Battery	Maximum state of charge	2 MW
	Minimum state of charge	0.2 MW
	Max. discharging/charging power	1 MW
	Dicharging/charging efficiency	0.77
AC subsystem		
Diesel generator	Maximum generation	1 MW
Wind turbine generator	Maximum generation	2 MW
Load	Maximum consumption	2 MW
Battery	Maximum state of charge	2 MW
	Minimum state of charge	0.2 MW
	Max. discharging/charging power	1 MW
	Dicharging/charging efficiency	0.77
Others		
Interlinking converter	Capacity	1 MVA
Transformer	Capacity	2 MVA

The loads in the modified system are timed by four to accommodate the augmented generation. The loads and renewable generation in the modified system are changing over the period based on their base capacities and corresponding daily profiles in Figure 5.

The coefficients in contribution model (11) and MG's operational mode (5) are chosen as shown in Table 4. Note that the cost coefficients can impact the solutions as well as the energy dispatch in MGs. Different sets of coefficients can be chosen

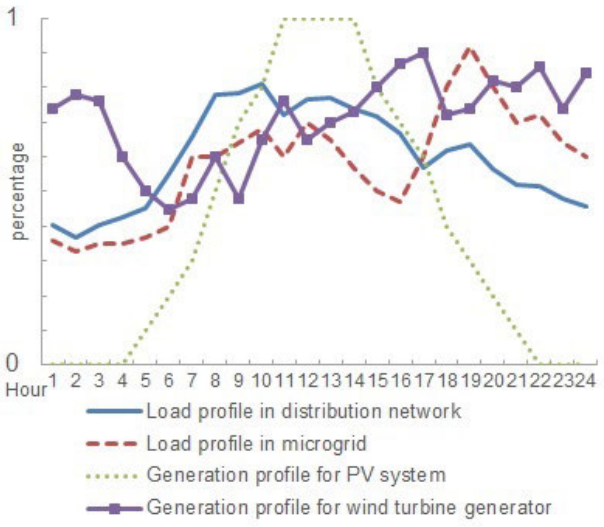

FIGURE 5. Profiles for loads and renewable generation.

TABLE 4. Cost coefficients chosen in this paper.

Coefficient	π	C_{dg}	C_{ess}	C_{rg}	C_{ad}
Value($)	1	0.6	0.5	-0.01	0.5

by DNO in a real system to accommodate its operational and economic interests.

For MOEA/D computation, the maximum iteration time is 100, and the population size R is set as 100. The number of closest neighbours T is 15. The crossover rate and mutation rate to be used in the genetic operator are 0.6 and 0.2, respectively. The reference vector z is initially filled with infinite negative values and iteratively updated by the maximal objective value discovered in each iteration.

B. ASSESSMENT OF VOLTAGE/VAR CONTROL PERFORMANCE

1) VOLTAGE QUALITY

Two comparative case studies are performed with and without VVC functionality to demonstrate the effectiveness of the proposed VVC. When the system operates without VVC functionality, all the renewable DGs maximise their active power generation, and their reactive power support are deactivated. Besides, the grid-tied MGs inject active power according to their operational model and disable their reactive power support. Figure 6 shows the hourly voltage quality index with and without activating the proposed VVC. The voltage quality index is calculated by (10), where V_{rated} and ΔV are 1 pu and 0.05 pu, respectively. The voltage quality index has been reduced significantly with VVC functionality as shown in Figure 6, which indicates that the voltage quality at all hours has been improved under the proposed VVC scheme.

To further assess the VVC performance, voltage profiles of some selected buses are illustrated in Figure 7. According to Figure 7b, voltage profiles at these buses are out of permitted range before activating VVC. The ending buses such as bus

FIGURE 6. Voltage quality index with and without VVC functionality.

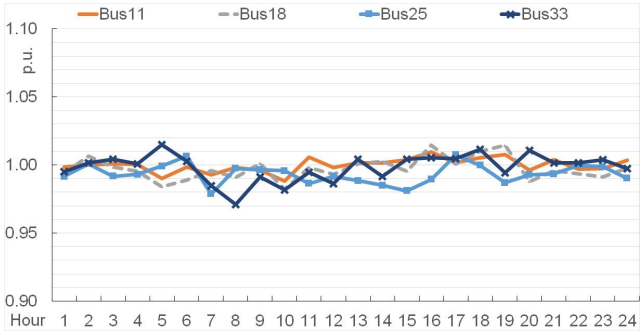

(a) Voltage profiles of selected buses with VVC

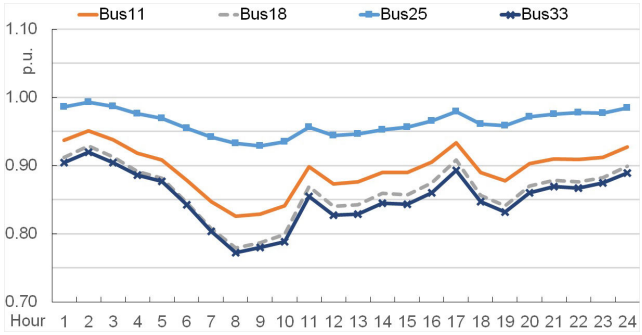

(b) Voltage profiles of selected buses without VVC

FIGURE 7. Voltage profiles of bus 11, 18, 25 and 33 with and without VVC functionality.

18 and 33 suffer from the worst voltage quality. After activating the proposed VVC, voltages at these buses are maintained within a secured range from 0.97 to 1.02 pu as observed in Figure 7a, even for the ending bus 18 and 33. It can be ascertained that the bus voltage profile in the system improves at all time after activating VVC functionality, which validates the superior performance of the proposed VVC scheme.

2) SETPOINTS OF VOLTAGE/VAR CONTROLLERS

In the proposed VVC, various controllers are coordinately scheduled. Their set-points are shown in Figure 8.

Figure 8a shows the secondary voltage of substation transformer. The OLTC controls the secondary voltage ranging from 0.98 to 1.05 pu. According to Figure 8a, OLTC maintains low tap positions during the night, while it is operated at relatively high tap positions during the daytime in response to the heavy load in the system.

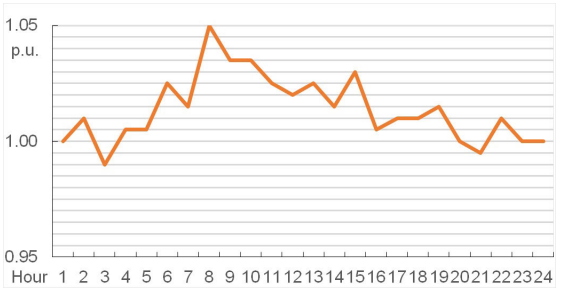

(a) Secondary voltage of substation transformer

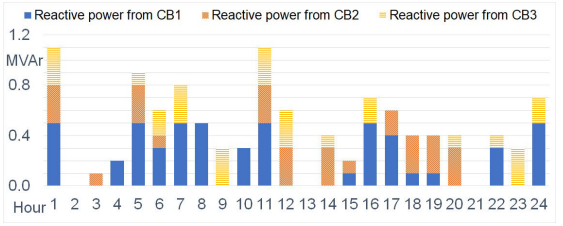

(b) Reactive power provided by capacitor banks

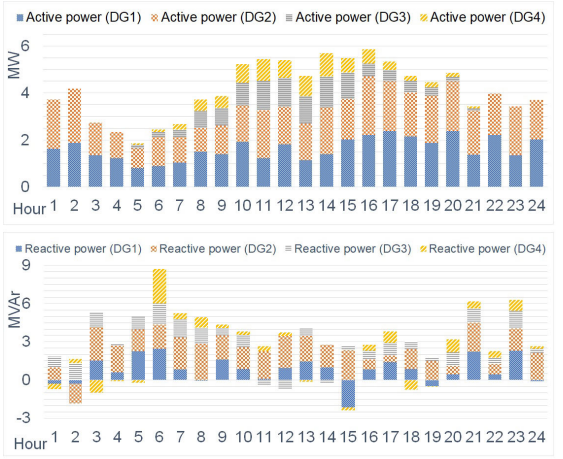

(c) Active and reactive power provided by distributed generators

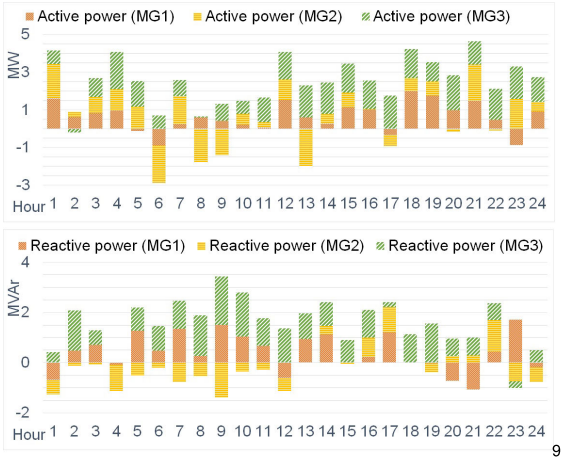

(d) Active and reactive power provided by hybrid ac/dc microgrids

FIGURE 8. Setpoints of various voltage/var resources.

Three CBs installed at bus 2, 24 and 30 are accordingly scheduled to provide reactive power compensation. Figure 8b shows the reactive power output of the CBs. It is worth

TABLE 5. Total active and reactive power generation of distributed generators and microgrids.

	Active power injection (MW)	Active power absorption (MW)	Reactive power injection (MVAr)	Reactive power absorption (MVAr)
DG1	39.329	0	22.136	3.327
DG2	40.703	0	41.061	1.546
DG3	11.353	0	18.292	1.437
DG4	7.998	0	10.039	2.876
MG1	17.738	2.209	13.372	3.379
MG2	15.429	8.026	3.937	8.026
MG3	29.693	0.188	22.891	0.273

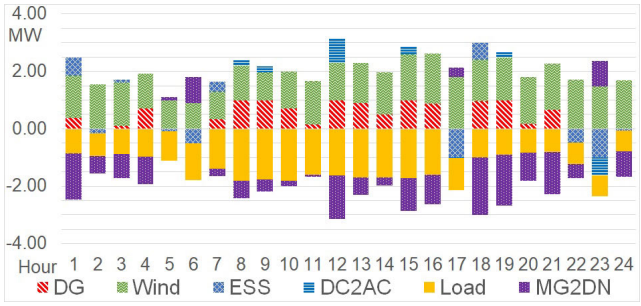

(a) Power balance in AC subsystem of microgrid 1

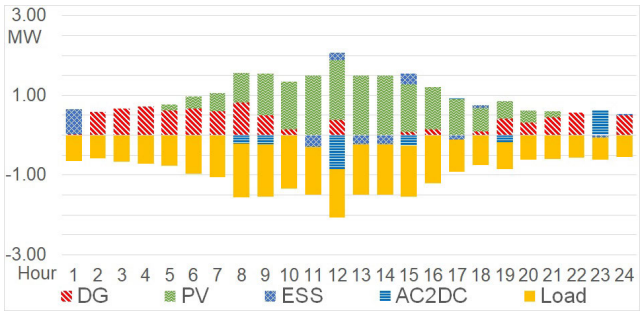

(b) Power balance in DC subsystem of microgrid 1

FIGURE 9. Power balance in microgrid 1.

mentioning that adjustment times of the mechanical controllers such as OLTC and CBs should be limited in a given period to save their lifetime. This kind of limit is not considered in this paper as the primary focus is to to seek trade-off solutions among various entities and fairly identify their contributions. Moreover, we believe that frequent adjustment may not be a problem if the system equips fully electronic devices.

In the proposed VVC model, the active power from renewable DGs can be modulated for power balance purpose, and their reactive power can be controlled to compensate reactive power shortage. Figure 8c shows the setpoints of the DGs. Table 5 shows the total active and reactive power provided by the DGs.

Figure 8d shows the active and reactive power provided by MGs. The MGs can either inject or absorb active power, which provides a superior capability to smooth the load variation in the distribution network. According to Figure 8d, three MGs respectively exchange active and reactive power with

the distribution network. Their total power exchange during the day is shown in Table 5.

3) POWER DISPATCH IN HYBRID AC/DC MG

In the proposed VVC scheme, the MOO model determines the power exchange between MGs and hybrid distribution network, while the setpoints of MG's local devices are determined by the operational model as proposed in II-C. In Figure 9, the power dispatch in MG1 is shown to assess the power dispatch in the grid-tied hybrid AC/DC MG. It can be observed that the renewable generation in the MG is always maximised. By contrast, the fuel-based diesel generators are strictly limited at all time, and the ESSs are only activated for limited hours to balance the load supply. The total operational costs of three MGs are 16.06 $, 16.80 $ and 22.88 $, respectively.

TABLE 6. Voltage/var control contributions provided by different voltage/var entities.

Hour	Voltage quality index	Voltage/Var control contribution ($)			
		DNO	MG1	MG2	MG3
1	2.376 (32.053)	3.138	14.139	1.655	10.745
2	2.512 (25.501)	3.927	11.738	0.355	6.970
3	3.097 (36.590)	2.442	17.472	0.871	12.707
4	1.854 (40.615)	4.125	13.230	1.719	19.687
5	4.385 (45.054)	5.460	11.592	2.959	20.658
6	4.912 (59.391)	21.586	6.273	6.157	20.463
7	5.897 (74.407)	16.371	22.518	6.133	23.488
8	8.813 (85.407)	33.763	18.225	5.682	18.923
9	6.564 (83.597)	24.745	23.842	1.436	27.010
10	9.278 (78.542)	22.801	17.555	3.958	24.950
11	5.639 (51.643)	15.664	7.711	1.758	20.871
12	5.268 (63.343)	14.784	14.815	1.666	26.810
13	4.856 (62.214)	14.586	18.071	0.212	24.489
14	4.697 (55.675)	9.807	15.420	1.700	24.052
15	6.571 (55.696)	13.921	14.027	0.899	20.278
16	4.269 (48.412)	4.747	14.715	2.908	21.773
17	3.151 (35.000)	5.676	6.623	2.088	17.462
18	4.659 (55.004)	3.875	24.008	1.485	20.977
19	5.798 (60.611)	8.367	22.859	2.279	21.308
20	3.053 (48.908)	5.124	9.831	4.373	26.526
21	2.766 (45.277)	3.727	12.078	5.527	21.179
22	3.152 (45.702)	6.846	12.241	1.778	21.685
23	2.121 (43.713)	7.193	7.356	6.826	20.217
24	2.620 (36.958)	3.015	11.809	2.110	17.403
Sum	108.31 (1269.31)	255.69	348.15	66.54	490.63

C. ASSESSMENT OF THE IDENTIFIED CONTRIBUTIONS

1) VOLTAGE/VAR CONTRIBUTIONS

There are four entities in the test system. Table 6 shows their contributions. The bracketed numbers in second column represent the hourly voltage quality index without VVC functionality. It can be observed in the last row of Table 6 that four entities help to reduce the daily voltage quality index from 1269.31 to 108.31. In response to their support, their shared contributions are 255.69 $, 348.15 $, 66.54 $ and 490.63 $, respectively. Moreover, it is noted that the contributions from hour 6 to hour 15 are relatively higher compared to other hours, which is due to that the loads during this period are heavy and downstream MGs' power support is effective in improving the voltage quality.

It is worth noting that the contributions of MG1 and MG3 are higher than MG2 at all time, although the parameters of their local loads and power generations are identical. The reason lies in that MG1 and MG3 are installed at heavy loaded buses and their power support can be more effective in improving the node voltage quality of neighbouring buses. This finding indicates that the location of an MG could impact its contributions. The optimum location of an MG from the perspective of VVC could be an essential factor that should be considered by MG's operator, which is out of scope for this paper and may require further investigation in our future studies.

2) IDENTIFICATION ACCURACY

To validate the identification accuracy, the data obtained at 2nd hour is selected as shown in Table 7. The total contribution at 2nd hour is 22.989, which is fairly distributed to the four entities by using the proposed identification terms as shown in the last row of Table 7. By contrast, using identification terms in the first and second row will generate mismatch in sharing the total contribution.

TABLE 7. Identification terms at 2nd hour.

	DNO	MG1	MG2	MG3	Sum
Contribution $C^1_{\omega_i}$ (when ith entity is the first to be added)	5.001	12.948	0.213	8.529	26.691
Contribution $C^4_{\omega_i}$ (when ith entity is the last to be added)	2.194	9.868	0.162	4.751	16.975
Contribution C_{ω_i} (when using the proposed identification approach)	3.927	11.738	0.355	6.970	22.989

VI. CONCLUSION

A multiobjective VVC model is proposed in this paper to seek tradeoff solutions for various entities to maximise their VVC contributions. The application of the multiobjective VVC model is supported by an identification method, which is developed based on the fair resource allocation theory. The proposed VVC controls not only the traditional controllers such as OLTC and CB but also the independent entities such as MGs. This feature extend its application scenario to the future hybrid distribution network where multiple entities with different operational interests coexist.

It was validated that the proposed VVC can securely maintain the voltage quality in hybrid distribution networks and it is capable of achieving optimised power supply in grid-tied hybrid AC/DC MGs at the same time. Moreover, the integrated identification approach in VVC scheme is capable of fairly identifying the contributions provided by different entities, which provides a promising solution for system operators to create an acceptable motivation plan to encourage the participation of different entities. Besides, the identification does not require the knowledge of entities' action sequences, which makes the proposed VVC viable to be used in practice.

REFERENCES

[1] A. Madureira and J. P. Lopes, "Coordinated voltage support in distribution networks with distributed generation and microgrids," *IET Renew. Power Gener.*, vol. 3, no. 4, p. 439, 2009.pp. 439–454,

[2] G. Joos, B. Ooi, D. Mcgillis, F. Galiana, and R. Marceau, "The potential of distributed generation to provide ancillary services," in *Proc. Power Eng. Soc. Summer Meeting*, Nov. 2002, pp. 1762–1767.

[3] Y. J. Kim, J. L. Kirtley, and L. K. Norford, "Reactive power ancillary service of synchronous dgs in coordination with voltage control devices," *IEEE Trans. Smart Grid*, vol. 8, no. 2, pp. 515–527, Sep. 2015.

[4] Y. Chai, L. Guo, C. Wang, Z. Zhao, X. Du, and J. Pan, "Network partition and voltage coordination control for distribution networks with high penetration of distributed PV units," *IEEE Trans. Power Syst.*, vol. 33, no. 3, pp. 3396–3407, May 2018.

[5] M. Chamana and B. H. Chowdhury, "Optimal voltage regulation of distribution networks with cascaded voltage regulators in the presence of high PV penetration," *IEEE Trans. Sustain. Energy*, vol. 9, no. 3, pp. 1427–1436, Jul. 2018.

[6] F. U. Nazir, B. C. Pal, and R. A. Jabr, "A two-stage chance constrained Volt/VAr control scheme for active distribution networks with nodal power uncertainties," *IEEE Trans. Power Syst.*, vol. 34, no. 1, pp. 314–325, Jan. 2019.

[7] R. A. Jabr, "Robust Volt/VAr control with photovoltaics," *IEEE Trans. Power Syst.*, vol. 34, no. 3, pp. 2401–2408, May 2019.

[8] R. P. Xu, C. Zhang, Y. Xu, and Z. Y. Dong, "Rolling horizon based multi-objective robust voltage/VAR regulation with conservation voltage reduction in high PV-penetrated distribution networks," *IET Gener., Transmiss. Distrib.*, vol. 13, no. 9, pp. 1621–1629, May 2019.

[9] L. Chen, Z. Deng, and X. Xu, "Two-stage dynamic reactive power dispatch strategy in distribution network considering the reactive power regulation of distributed generations," *IEEE Trans. Power Syst.*, vol. 34, no. 2, pp. 1021–1032, Mar. 2019.

[10] J. Vasquez, R. Mastromauro, J. Guerrero, and M. Liserre, "Voltage support provided by a droop-controlled multifunctional inverter," *IEEE Trans. Ind. Electron.*, vol. 56, no. 11, pp. 4510–4519, Nov. 2009.

[11] K. Turitsyn, P. Sulc, S. Backhaus, and M. Chertkov, "Options for control of reactive power by distributed photovoltaic generators," *Proc. IEEE*, vol. 99, no. 6, pp. 1063–1073, Jun. 2011.

[12] V. Calderaro, G. Conio, V. Galdi, G. Massa, and A. Piccolo, "Optimal decentralized voltage control for distribution systems with inverter-based distributed generators," *IEEE Trans. Power Syst.*, vol. 29, no. 1, pp. 230–241, Jan. 2014.

[13] X. Wang, C. Wang, T. Xu, H. Meng, P. Li, and L. Yu, "Distributed voltage control for active distribution networks based on distribution Phasor measurement units," *Appl. Energy*, vol. 229, pp. 804–813, Nov. 2018.

[14] L. Wang, F. Bai, R. Yan, and T. K. Saha, "Real-time coordinated voltage control of PV inverters and energy storage for weak networks with high PV penetration," *IEEE Trans. Power Syst.*, vol. 33, no. 3, pp. 3383–3395, May 2018.

[15] Y. Zheng, D. J. Hill, K. Meng, and S. Y. Hui, "Critical bus voltage support in distribution systems with electric springs and responsibility sharing," *IEEE Trans. Power Syst.*, vol. 32, no. 5, pp. 3584–3593, Sep. 2017.

[16] A. Borghetti, R. Bottura, M. Barbiroli, and C. A. Nucci, "Synchrophasors-based distributed secondary voltage/VAR control via cellular network," *IEEE Trans. Smart Grid*, vol. 8, no. 1, pp. 262–274, Jan. 2017.

[17] J. Ding, Q. Zhang, S. Hu, Q. Wang, and Q. Ye, "Clusters partition and zonal voltage regulation for distribution networks with high penetration of PVs," *IET Gener., Transmiss. Distrib.*, vol. 12, no. 22, pp. 6041–6051, Dec. 2018.

[18] Y. Wang, Y. Xu, Y. Tang, M. H. Syed, E. Guillo-Sansano, and G. M. Burt, "Decentralised-distributed hybrid voltage regulation of power distribution networks based on power inverters," *IET Gener., Transmiss. Distrib.*, vol. 13, no. 3, pp. 444–451, Feb. 2019.

[19] M. Zeraati, M. E. Hamedani Golshan, and J. M. Guerrero, "A consensus-based cooperative control of PEV battery and PV active power curtailment for voltage regulation in distribution networks," *IEEE Trans. Smart Grid*, vol. 10, no. 1, pp. 670–680, Jan. 2019.

[20] I. N. Kouveliotis-Lysikatos, D. I. Koukoula, and N. D. Hatziargyriou, "A double-layered fully distributed voltage control method for active distribution networks," *IEEE Trans. Smart Grid*, vol. 10, no. 2, pp. 1465–1476, Mar. 2019.

[21] H. J. Liu, W. Shi, and H. Zhu, "Hybrid voltage control in distribution networks under limited communication rates," *IEEE Trans. Smart Grid*, vol. 10, no. 3, pp. 2416–2427, May 2019.

[22] X. Wang, C. Wang, T. Xu, L. Guo, S. Fan, and Z. Wei, "Decentralised voltage control with built-in incentives for participants in distribution networks," *IET Gener., Transmiss. Distrib.*, vol. 12, no. 3, pp. 790–797, 2017.

[23] X. Dou, P. Xu, Q. Hu, W. Sheng, X. Quan, Z. Wu, and B. Xu, "A distributed voltage control strategy for multi-microgrid active distribution networks considering economy and response speed," *IEEE Access*, vol. 6, pp. 31259–31268, 2018.

[24] X. Liu, P. Wang, and P. C. Loh, "A hybrid AC/DC microgrid and its coordination control," *IEEE Trans. Smart Grid*, vol. 2, no. 2, pp. 278–286, Jun. 2011.

[25] M. Baran, V. Banunarayanan, and K. Garren, "A transaction assessment method for allocation of transmission services," *IEEE Trans. Power Syst.*, vol. 14, no. 3, pp. 920–928, Aug. 1999.

[26] T. Ibaraki and N. Katoh, *Resource Allocation Problems: Algorithmic Approaches*. Cambridge, MA, USA: MIT Press, 1988.

[27] K. Deb, "Multi-objective optimization," in *Search Methodologies*. Boston, MA, USA: Springer, 2014, pp. 403–449.

[28] A. M. Jubril, O. A. Komolafe, and K. O. Alawode, "Solving multi-objective economic dispatch problem via semidefinite programming," *IEEE Trans. Power Syst.*, vol. 28, no. 3, pp. 2056–2064, Aug. 2013.

[29] Q. Zhang and H. Li, "MOEA/D: A multiobjective evolutionary algorithm based on decomposition," *IEEE Trans. Evol. Comput.*, vol. 11, no. 6, pp. 712–731, Dec. 2007.

[30] K. Deb, A. Pratap, S. Agarwal, and T. Meyarivan, "A fast and elitist multiobjective genetic algorithm: NSGA-II," *IEEE Trans. Evol. Comput.*, vol. 6, no. 2, pp. 182–197, Apr. 2002.

[31] A. Jaszkiewicz, "On the performance of multiple-objective genetic local search on the 0/1 knapsack problem–a comparative experiment," *IEEE Trans. Evol. Comput.*, vol. 6, no. 4, pp. 402–412, Aug. 2002.

[32] X. Blasco, J. Herrero, J. Sanchis, and M. Martínez, "A new graphical visualization of n-dimensional Pareto front for decision-making in multiobjective optimization," *Inf. Sci.*, vol. 178, no. 20, pp. 3908–3924, Oct. 2008.

[33] C.-J. Ye and M.-X. Huang, "Multi-objective optimal power flow considering transient stability based on parallel NSGA-II," *IEEE Trans. Power Syst.*, vol. 30, no. 2, pp. 857–866, Mar. 2015.

[34] A. G. Di Nuovo, M. Palesi, D. Patti, G. Ascia, and V. Catania, "Fuzzy decision making in embedded system design," in *Proc. 4th Int. Conf. Hardw./Softw. Codesign Syst. Synth. (CODES+ISSS)*, 2006, pp. 223–228.

[35] M. E. Baran and F. F. Wu, "Network reconfiguration in distribution systems for loss reduction and load balancing," *IEEE Power Eng. Rev.*, vol. 9, no. 4, pp. 101–102, Apr. 1989.

FENG QIAO (Student Member, IEEE) received the B.S. degree from Northeast Dianli University, in 2011, and the M.S. degree from North China Electric Power University, in 2014, both in electrical engineering. He is currently pursuing the Ph.D. degree in electrical engineering with the School of Electrical and Information Engineering, The University of Sydney. His research interests include optimization-based voltage/var control and data-driven strategies in improving voltage quality in hybrid ac/dc distribution networks.

JIN MA (Member, IEEE) received the B.S. and M.S. degrees in electrical engineering from Zhejiang University, Hangzhou, China, in 1997 and 2000, respectively, and the Ph.D. degree in electrical engineering from Tsinghua University, Beijing, China, in 2004. He is currently with the School of Electrical and Information Engineering, The University of Sydney. His major research interests are load modeling, nonlinear control systems, dynamic power systems, and power system economics. He is a member of CIGRE W.G. C4.605 Modeling and aggregation of loads in flexible power networks and the Corresponding Member of CIGRE Joint Workgroup C4-C6/CIRED Modeling and dynamic performance of inverter-based generation in power system transmission and distribution studies. He is a registered Chartered Engineer.